# An investigation on microphysical characteristics of early-, late-, and post-Mei-yu season rainfall over Taiwan




## Balaji Kumar Seela

**Balaji Kumar Seela, Jayalakshmi Janapati, and Pay-Liam Lin***

Planetary Boundary Layer and Air pollution Laboratory (PBLAP)
Department of Atmospheric Sciences, National Central University, Taiwan

# Introduction

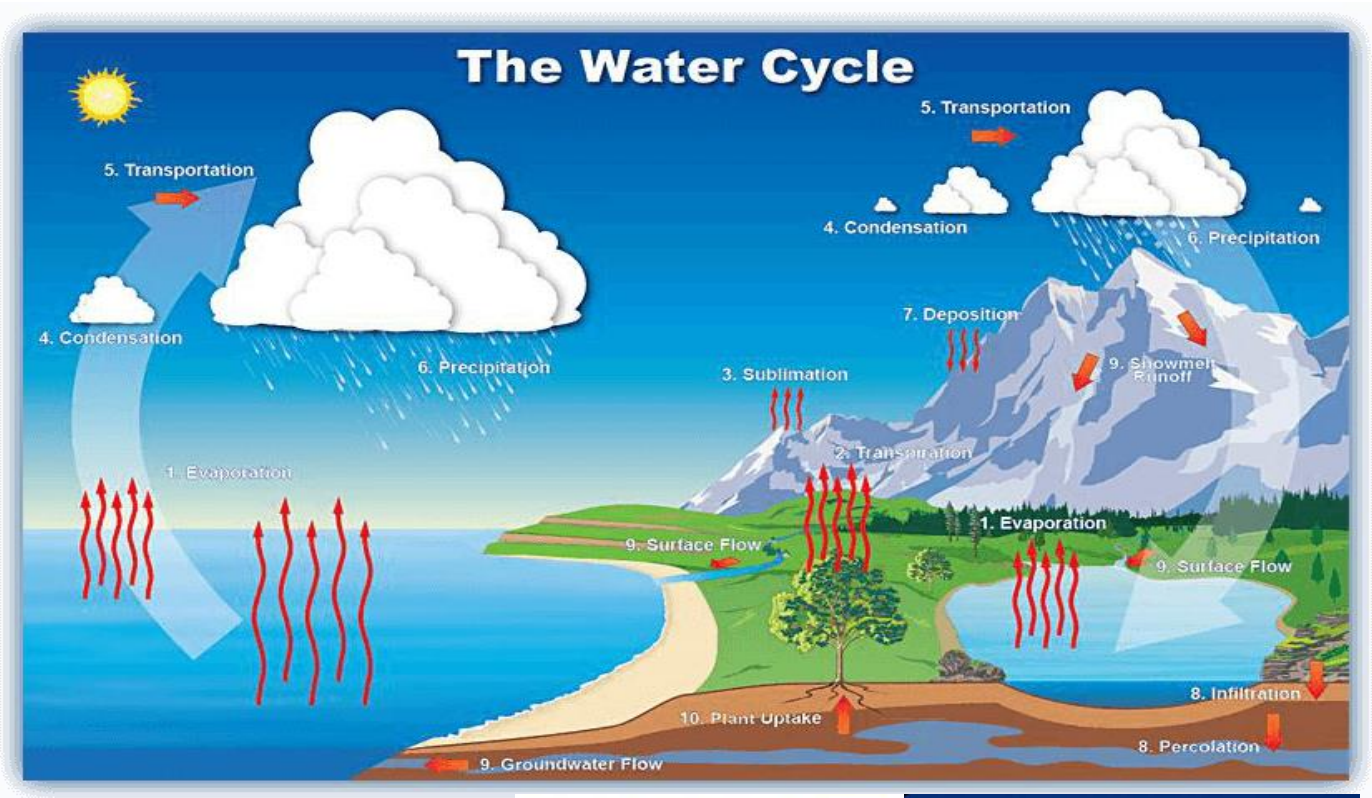


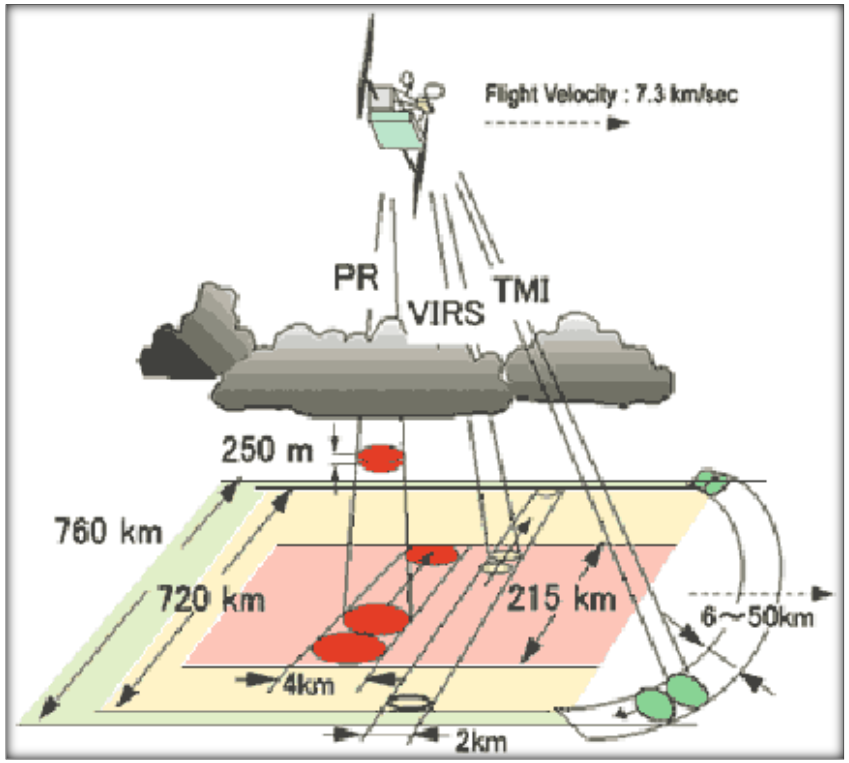



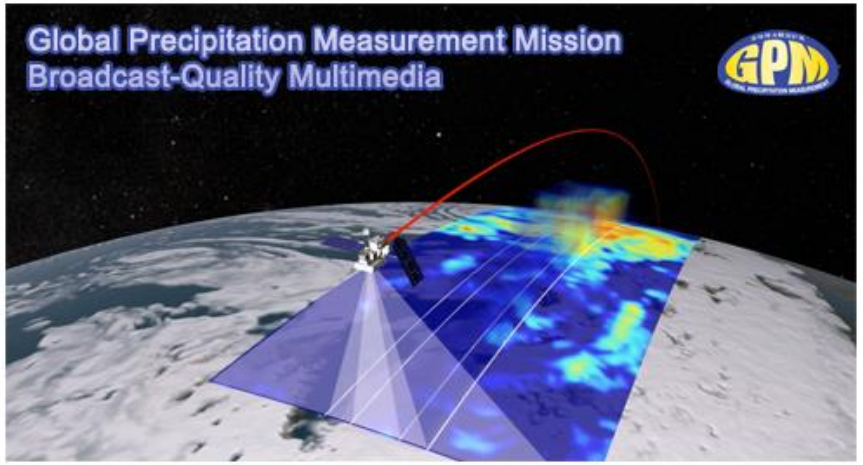

# **GPM DPR:** global precipitation measurement mission dual-frequency precipitation radar

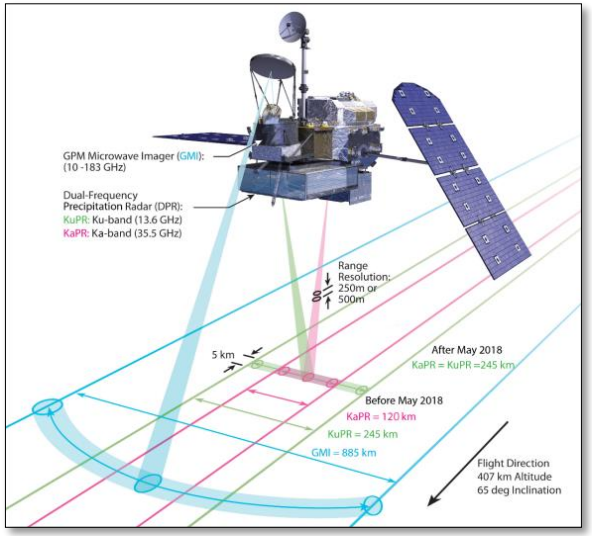


| System | KuPR | KaPR |
|---|---|---|
| Swath Width | 245 kilometers (km) | 245 kilometers (km) as of May 2018 (previously 120km) |
| Range Resolution | 250 meters (m) | 250/500 meters (m) |
| Spatial Resolution | 5 km (Nadir) | 5 km (Nadir) |
| Beam Width | 0.71 degrees | 0.71 degrees |
| Transmitter | 128 Solid State Amplifiers | 128 Solid State Amplifiers |
| Peak Transmit Power | 1013 Watts (W) | 146 Watts (W) |
| Pulse Repetition Freq. (In nominal operations mode) | 4100 to 4400 Hertz | 4100 to 4400 Hertz |
| Pulse Width | two 1.667 microseconds (µs) pulses | two 1.667 microseconds (µs) pulses in matched beams two 3.234 microseconds (µs) pulses in interlaced scans |
| Beam Number | 49 | 49 (25 in matched beams and 24 in interlaced scans) |

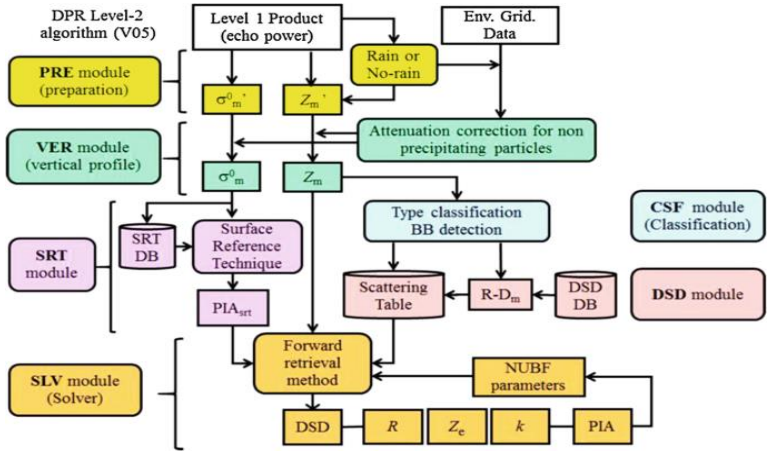


**Fig.:** GPM DPR algorithm

$R$ ( mm $h^{-1}$)

$Z_{ku/Ka}$ (dBZ)

$D_m$ (mm)

$dBN_w$ ($m^{-3}$ $mm^{-1}$)

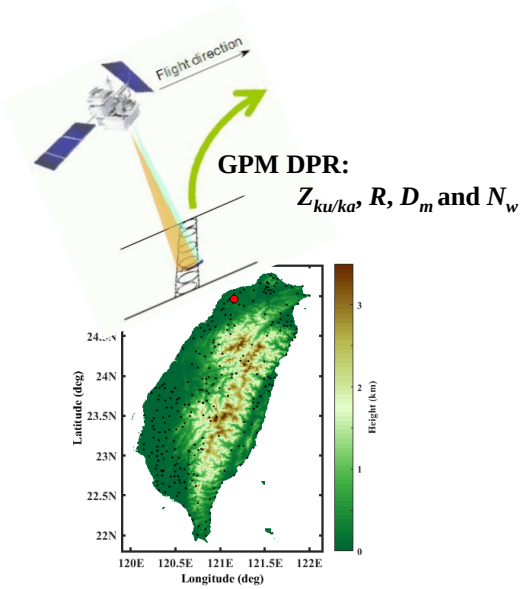


**Study period:**

Years**: 2014-2023**

Mei-yu**: May-June**

early-Mei-yu: 16-31 May

late-Mei-yu: 01 -15 June

post-Mei-Yu: 16 -31 June

# Results & Discussion

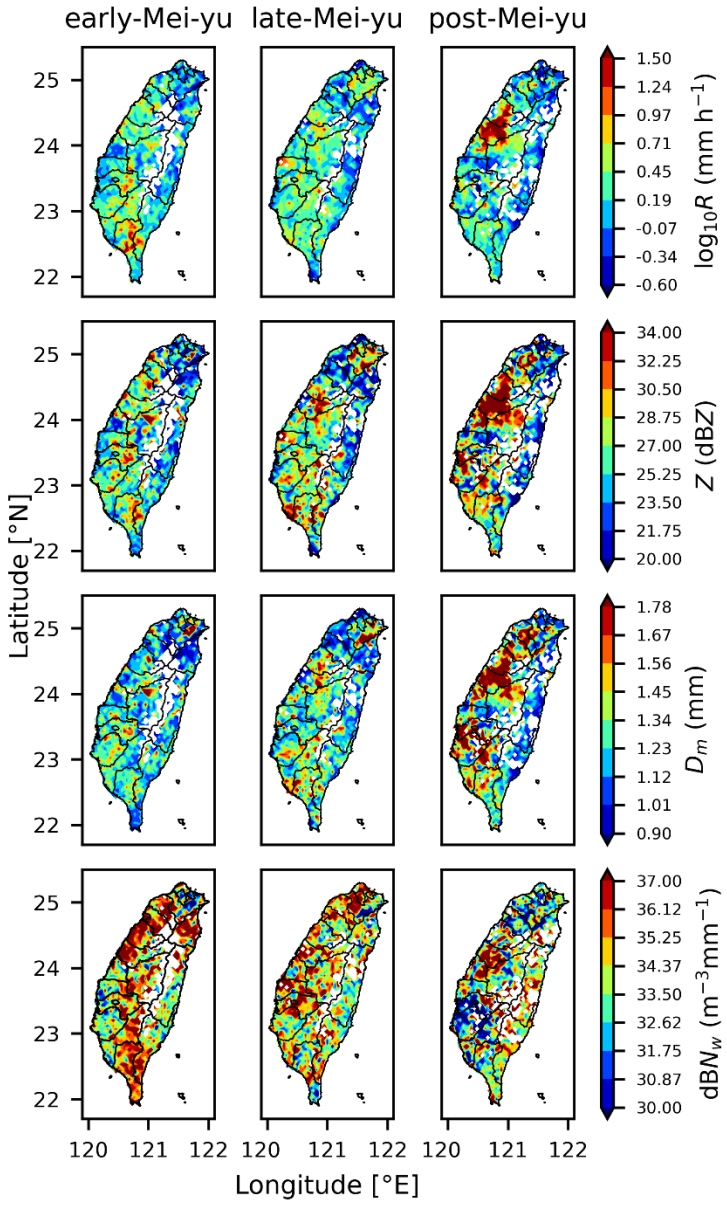


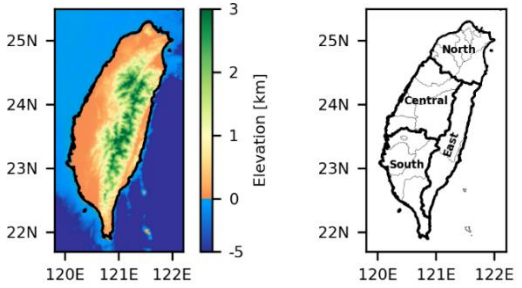


**Fig.** Spatial distribution of near-surface (2 km) (a) precipitation rate ($R$, mm h$^{-1}$), (b) radar reflectivity ($Z$, dBZ), (c) mass-weighted mean diameter ($D_m$, mm), (d) normalized intercept parameter (dB$N_w$:10log$_{10}N_w$, $N_w$ in m$^{-3}$ mm$^{-1}$) for early-, late-, and post-Mei-yu rainfall over Taiwan.

# Results & Discussion

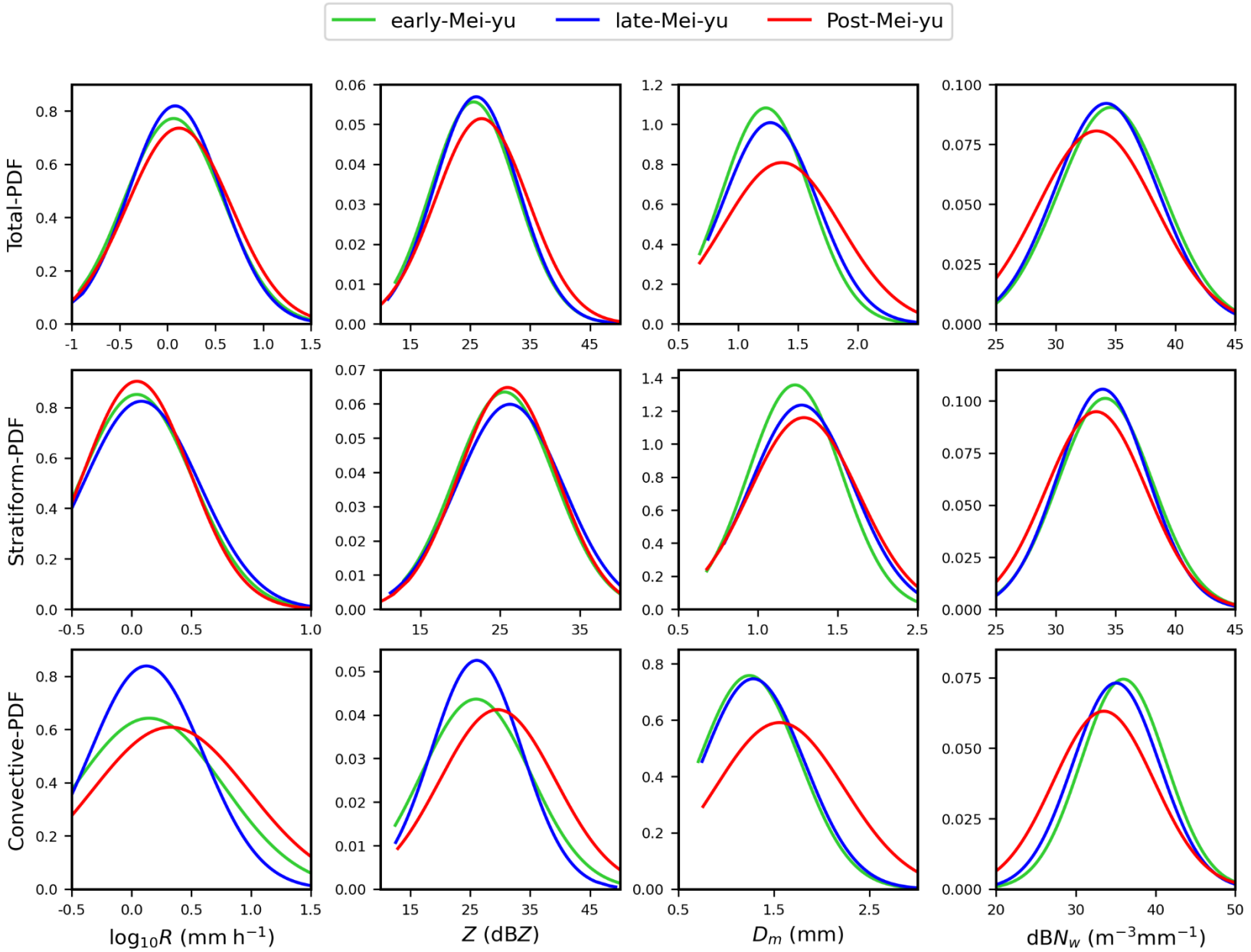


**Fig.** Probability density function (PDF) of near-surface (2 km) rainfall rate ($R$, mm $h^{-1}$) (first column), radar reflectivity ($Z$, dBZ), mass-weighted mean diameter ($D_m$, mm), and normalized intercept parameter (dB$N_w$: $10\log_{10}N_w$, $N_w$ in $m^{-3}$ $mm^{-1}$) for early-, late-, and post-Mei-yu rainfall.

# Results & Discussion

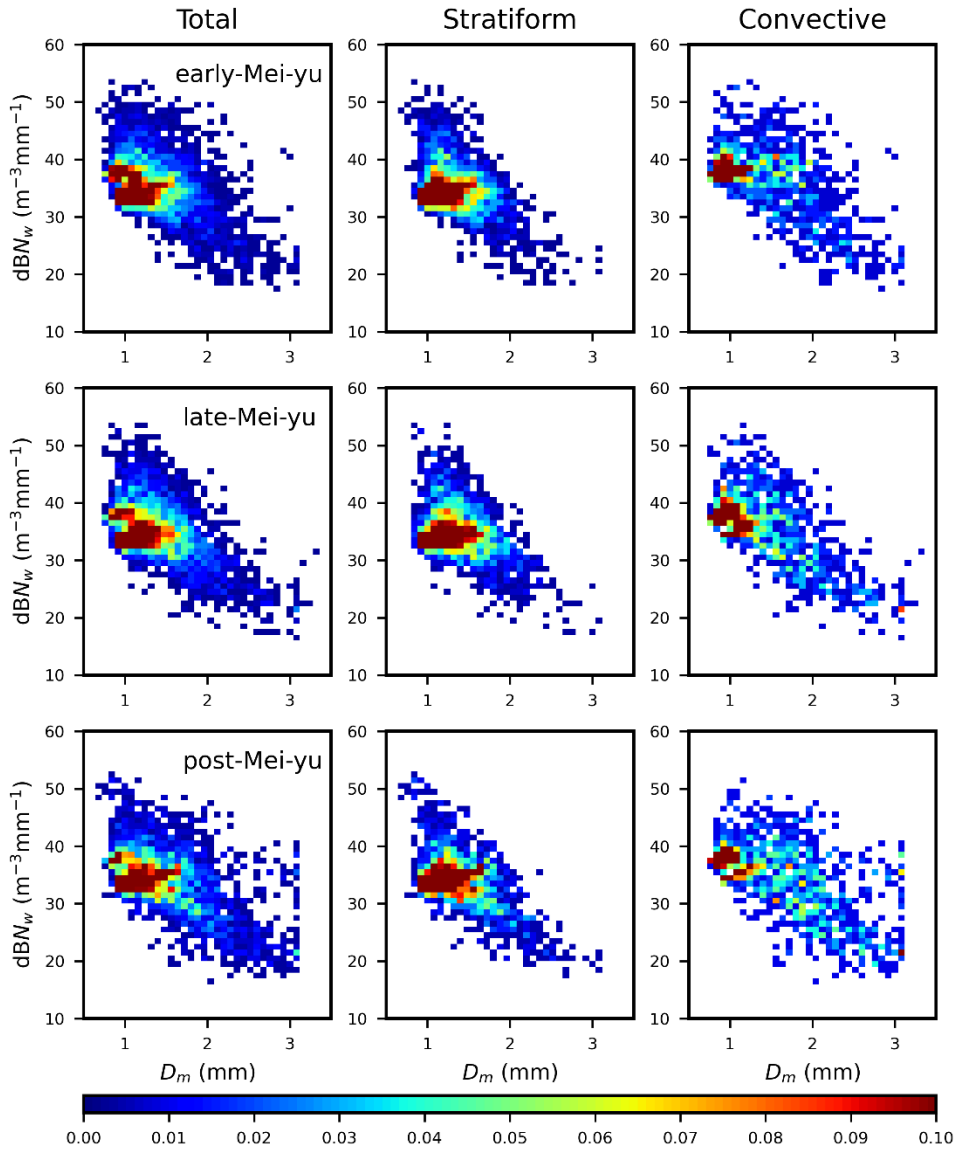


**Fig.** Two dimensional histogram between the near-surface (2 km) mass-weighted mean diameter ($D_m$, mm) and normalized intercept parameter (dB$N_w$: $10\log_{10}N_w$, $N_w$ in $m^{-3}$ $mm^{-1}$) for early-, late-, and post-Mei-yu rainfall.

# Results & Discussion

## CFAD: Total rainfall

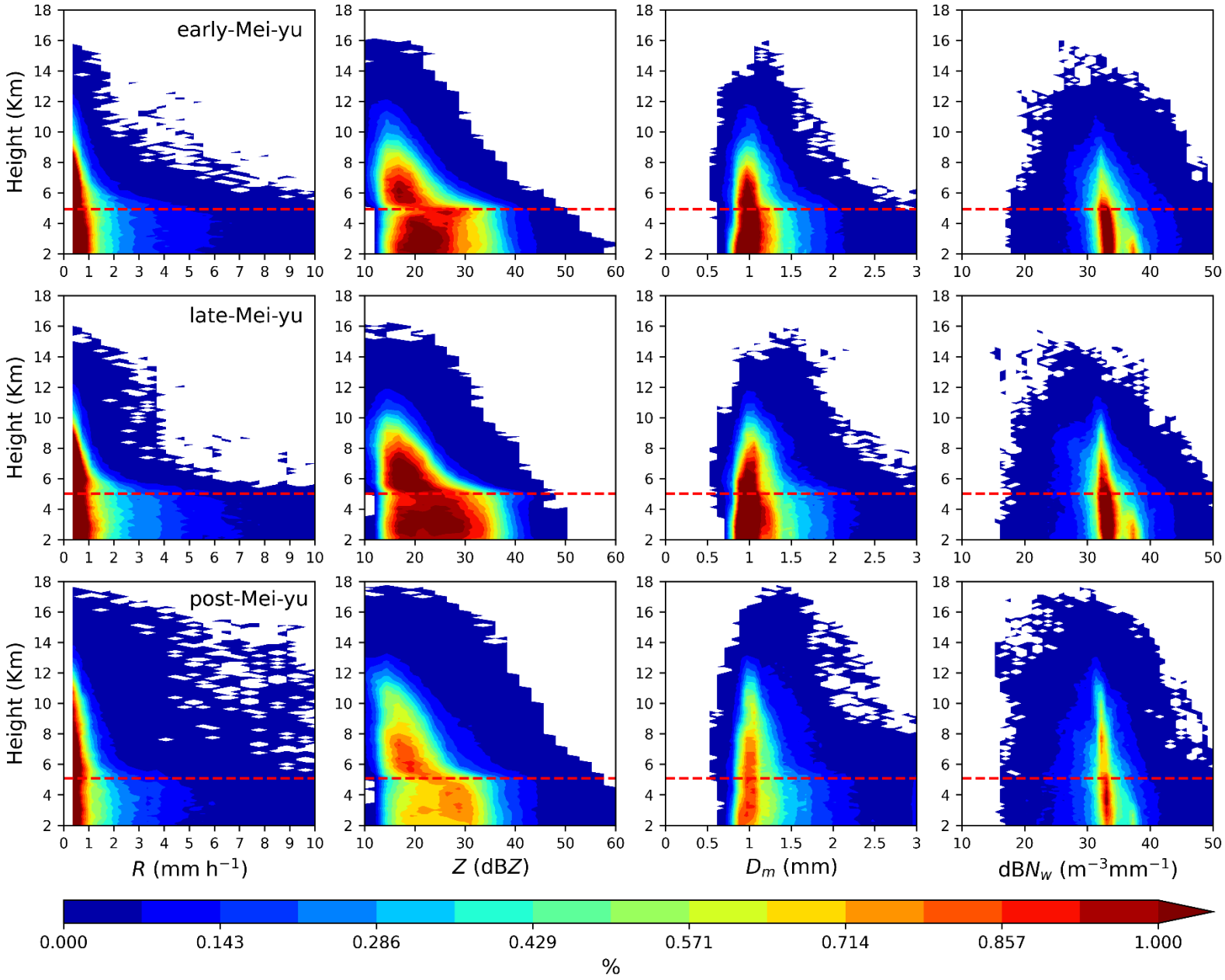


**Fig.** Contour frequency by altitude diagram (CFAD) of $R$ (mm h$^{-1}$), $Z$ (dBZ), $D_m$ (mm) dB$N_w$ (10log$_{10}N_w$, $N_w$ in m$^{-3}$ mm$^{-1}$) for early-, late-, and post-Mei-yu ***total rainfall*** .

# Results & Discussion

## CFAD: Stratiform rainfall

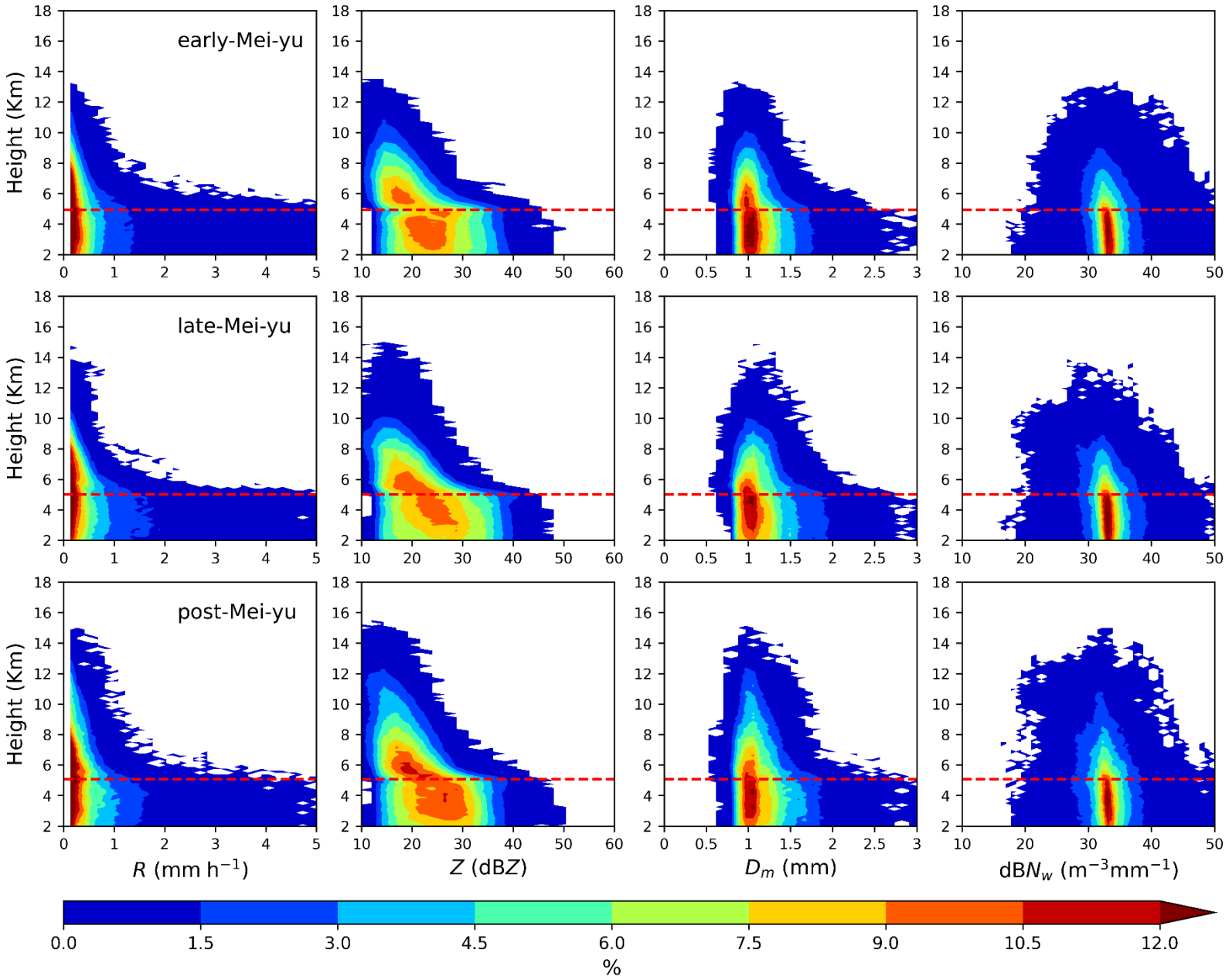


**Fig.** Contour frequency by altitude diagram (CFAD) of $R$ (mm h$^{-1}$), $Z$ (dBZ), $D_m$ (mm) dB$N_w$ (10log$_{10}N_w$, $N_w$ in m$^{-3}$ mm$^{-1}$) for early-, late-, and post-Mei-yu ***stratiform rainfall*** .

# Results & Discussion

## CFAD: Convective rainfall

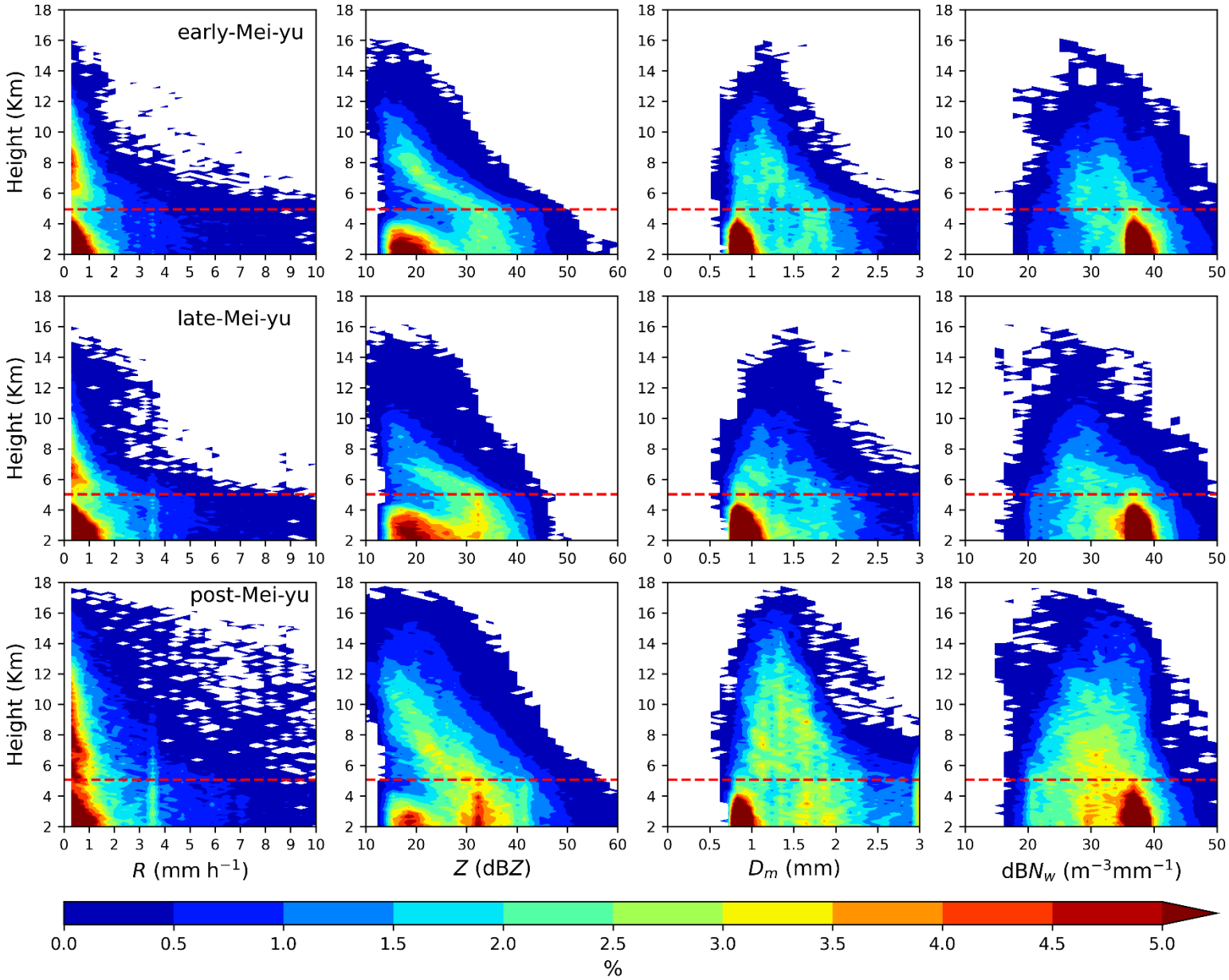


**Fig.** Contour frequency by altitude diagram (CFAD) of $R$ (mm h$^{-1}$), $Z$ (dBZ), $D_m$ (mm) dB$N_w$ (10log$_{10}N_w$, $N_w$ in m$^{-3}$ mm$^{-1}$) for early-, late-, and post-Mei-yu ***convective rainfall*** .

# Results & Discussion

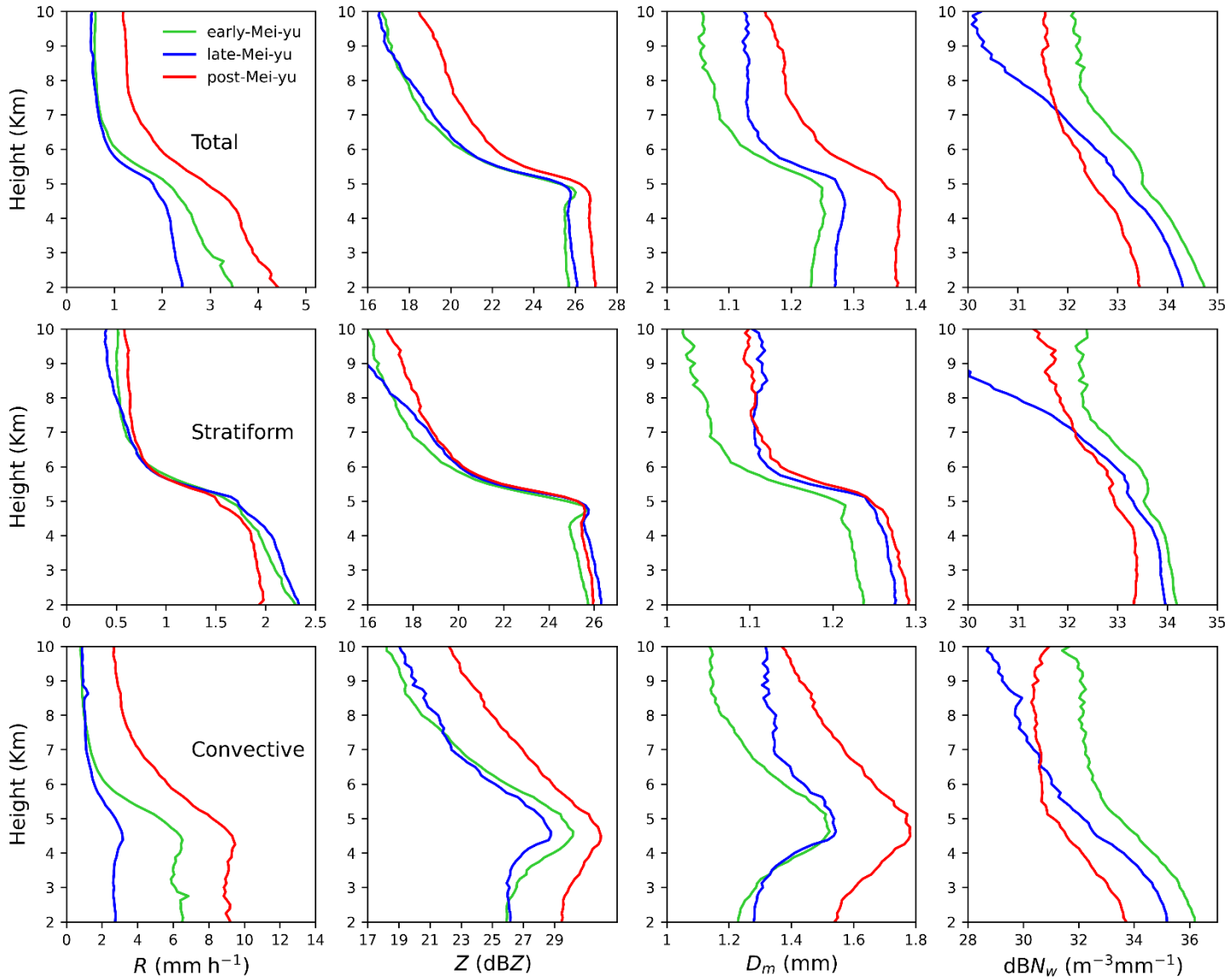


**Fig.** Mean profiles of $R$ (mm h$^{-1}$), $Z$ (dBZ), $D_m$ (mm) dB$N_w$ ($10\log_{10}N_w$, $N_w$ in m$^{-3}$ mm$^{-1}$) early-, late-, and post-Mei-yu *rainfall* .

# Results & Discussion

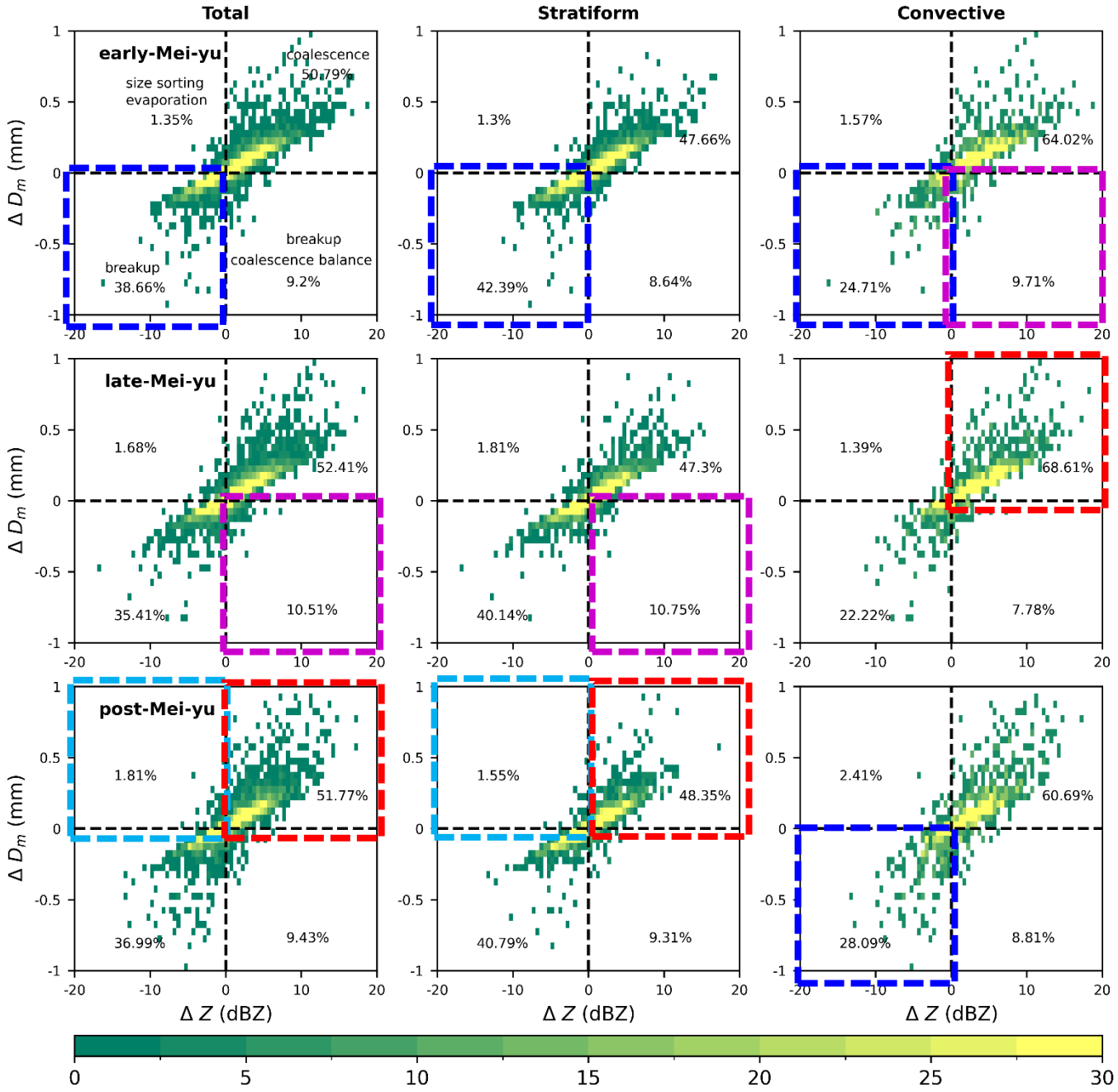


**Fig.** Probability density distributions of mass-weighted mean diameter and radar reflectivity in the 1 km layer depth ($\Delta D_m=(D_m)_{2\ \mathrm{km}}-(D_m)_{3\ \mathrm{km}}$ and $\Delta Z=(Z)_{2\ \mathrm{km}}-(Z)_{3\ \mathrm{km}}$) in the warm rain regions early-, late-, and post-Mei-yu season rainfall.

# Results & Discussion

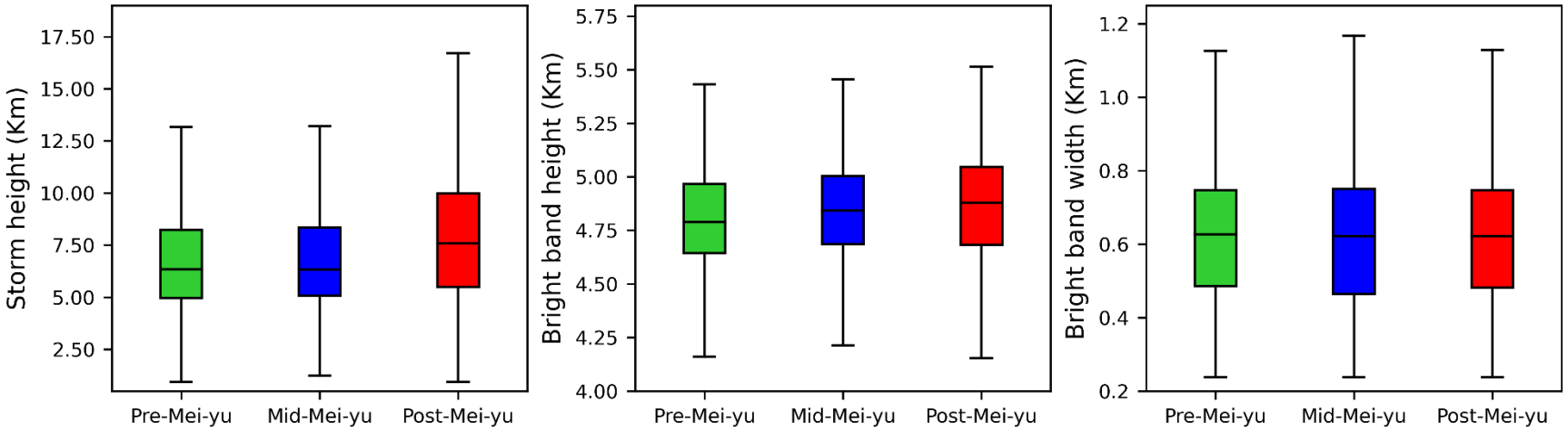


**Fig.** Storm heights , bright band heights and bright band widths of early-, late-, and post-Mei-yu seasons.

# Conclusions

- Rainfall rates → post-mei-yu > early- and late-mei-yu (total and convective precipitation).
- The echo top heights → post-mei-yu > early- and late-mei-yu.
- Small drops concentration → early-Mei-yu > late- and post-Mei-yu
- Warm rain processes:
  - Size sorting-evaporation processes: Post-Mei-yu (total and convective)
  - Breakup process : early-Mei-yu (total, stratiform, and convective)
    Post-Mei-yu (convective)

    collision-coalescence processes: late-Mei-yu (convective)
    post-Mei-yu (total and stratiform)
  - Collision-coalescence and breakup balance : early-Mei-yu (convective)
    late-Mei-yu (total and stratiform)
- Dominant size sorting and evaporation processes in post-mei-yu (total and convective) →more bigger size drops
- Predominance of breakup process in early-mei-yu (total and stratiform) rainfall resulted in more small-size drops.

JGR Atmospheres

RESEARCH ARTICLE
10.1029/2024JD040847

# An Investigation on Microphysical Characteristics of Early-, Late-, and Post-Mei-yu Season Rainfall Over Taiwan

**Balaji Kumar Seela[1], Jayalakshmi Janapati[1], Pay-Liam Lin[1,2,3], Chian-Yi Liu[4], and Chuan-Chi Tu[1]**

[1]Department of Atmospheric Sciences, Institute of Atmospheric Physics, National Central University, Taoyuan City, Taiwan, [2]Earthquake-Disaster and Risk Evaluation and Management Center, National Central University, Taoyuan City, Taiwan, [3]Research Center for Hazard Mitigation and Prevention, National Central University, Taoyuan City, Taiwan, [4]Research Centre for Environmental Changes, Academia Sinica, Taipei, Taiwan

**Key Points:**

- Investigations on the microphysical attributes of early-Mei-yu, late-Mei-yu, and post-Mei-yu over Taiwan using GPM DPR showed distinctions among these three sub-seasons
- As the sub-season transitioned from early-Mei-yu to post-Mei-yu, the shift from heavy rainfall in the south to the central region of Taiwan became evident
- The dominant breakup process (breakup, size-sorting, and evaporation processes) in early-Mei-yu (post-Mei-yu) resulted in lower (higher) rainfall amounts than in the late- and post-Mei-yu seasons

**Correspondence to:**

P.-L. Lin,
tliam@pblap.atm.ncu.edu.tw

**Citation:**

Seela, B. K., Janapati, J., Lin, P.-L., Liu, C.-Y., & Tu, C.-C. (2024). An investigation on microphysical characteristics of early-, late-, and post-Mei-yu season rainfall over Taiwan. *Journal of Geophysical Research: Atmospheres*, *129*, e2024JD040847. https://doi.org/10.1029/2024JD040847

Received 21 JAN 2024
Accepted 5 AUG 2024

**Author Contributions:**

**Conceptualization:** Balaji Kumar Seela, Jayalakshmi Janapati, Pay-Liam Lin, Chian-Yi Liu
**Data curation:** Pay-Liam Lin

**Abstract** Over Taiwan, Mei-yu season (May and June), which is primarily linked to frontal systems, is the transition period between winter and summer. Using the Global Precipitation Measurement Mission dual-frequency precipitation radar (GPM DPR), the current study examined the rain and microphysical characteristics of the Mei-yu season in Taiwan. In order to examine the areal and intra-seasonal aspects, May and June months are divided into three sub-seasons: early-Mei-yu, late-Mei-yu, and post-Mei-yu. The three sub-seasons exhibited differences in rainfall and raindrop size distributions, with abundance of large drops in the post-Mei-yu. Additionally, there were noticeable variations in the raindrop size distributions among the south, central, north, and eastern parts of Taiwan, with more large drops in central Taiwan. To comprehend the microphysical progressions causing the regional and intra-seasonal fluctuations, CFADs (contoured frequency by altitude diagrams) of rain parameters are utilized. Compared to other two sub-seasons, the early-Mei-yu season exhibited weaker convection. Dominance of stratiform precipitation in late-Mei-yu season, and convective precipitation in post-Mei-yu season resulted in higher rainfall amounts in these two sub-seasons (more particularly in post-Mei-yu) than the early-Mei-yu season. Examination of warm rain microphysical processes (below 5 km height) among these sub-seasons revealed that the early-Mei-yu season is dominated with break-up process, late-Mei-yu season with breakup and coalescence balance, and post-Mei-yu with coalescence, size-sorting and evaporation processes.

**Plain Language Summary** Significant socioeconomic effects of Mei-yu season rainfall over Taiwan compelled for the improved understanding of precipitating cloud systems in Mei-yu season. The microphysical attributes of Mei-yu season rainfall are investigated in terms of spatial and sub-seasonal scale (early-Mei-yu, late-Mei-yu, and post-Mei-yu) using GPM DPR estimates. The results demonstrated that the spatial distributions of rainfall amounts shifts from south to central Taiwan with the progress (early-Mei-yu to post-Mei-yu) of the season. Early-Mei-yu season with weaker convection and break-up processes exhibit lower rainfall amount than late-, and post-Mei-yu season. On the contrary, the post-Mei-yu season with strong convection, coalescence, size-sorting and evaporation processes showed higher rainfall amounts over early-


# *Thank you for your attention.*